Global Journal of Researches in Engineering: E
Civil And Structural Engineering
Volume 24 Issue 1 Version 1.0 Year 2024
Type: Double Blind Peer Reviewed International Research Journal
Publisher: Global Journals
Online ISSN: 2249-4596 & Print ISSN: 0975-5861

Enhancement of Cement's Compressive Strength of Concrete using Mid-Infrared Ray – A Fundamental Research

By Umakanthan T, Madhu Mathi & Umadevi U

Abstract- Concrete is one of the most versatile material in building construction. Overall quality of cement is indicated by the compressive concrete strength of concrete (CSC). Many techniques are available to increase the CSC. As one of the technology, we irradiated the cement with mid-infrared rays and observed 38% CSC increase. This technology is economical, rapid, easy, user-friendly, can be used by manufacturer to client and in future may gain vast scope and utility in civil engineering.

Keywords: *cement, mid-infrared, irradiation, compressive strength of concrete, increase, safe, economical.*

GJRE-E Classification: *FOR Code: 0905*

Strictly as per the compliance and regulations of:

Enhancement of Cement's Compressive Strength of Concrete using Mid-Infrared Ray – A Fundamental Research

Umakanthan T [α], Madhu Mathi [σ] & Umadevi U [ρ]

Abstract- **Concrete is one of the most versatile material in building construction. Overall quality of cement is indicated by the compressive concrete strength of concrete (CSC). Many techniques are available to increase the CSC. As one of the technology, we irradiated the cement with mid-infrared rays and observed 38% CSC increase. This technology is economical, rapid, easy, user-friendly, can be used by manufacturer to client and in future may gain vast scope and utility in civil engineering.**

Keywords: cement, mid-infrared, irradiation, compressive strength of concrete, increase, safe, economical.

I. Introduction

About 10 billion tons of concrete used leading to natural resource decline, and increasing pollution hence research for alternative needed *(Liu et al., 2020)*. Cement price and demand are dynamic. Either saving atleast 1% of cement or increasing the compressive strength of concrete (CSC) would save economy and reduce pollution. CSC is influenced by type and source of cement, supplementary cementitious material and aggregate type *(Jared et al., 2022)*. Through various research CSC was increased upto 72.3% as cited by Liu *et al*., 2020. Most of these methods are unstable, uneconomical and difficult to follow in field conditions. We successfully tried mid-infrared irradiation and found 38% CSC increase. The effect of mid-infrared in cement's physic-chemistry is also discussed with various instrumentations.

II. Material and Methods

MIRGA *(patent no.: 401387)* is a 20 ml pocket sized atomizer *(Supplementary file – figure F1)* containing inorganic water based solution in which approximately two sextillion cations and three sextillion anions composing Sodium carbonate monohydrate, Sodium carbonate anhydrous, Potassium nitrate and Sodium chloride are present. During spraying, depending on pressure (vary with the user) applied to plunger, every spraying generates 2-6 μm mid-IR. Design of the MIRGA and emission of 2-6 μm mid-IR has been presented in detail by *Umakanthan et al., 2022a; Umakanthan et al., 2022b*. Every time spraying emits 0.06ml which contains approximately seven quintillion cations and eleven quintillion anions. *(details about MIRGA available in supplementary text T1)*

The inorganic compounds used in the generation of MIR are a perspective for biomedical applications *(Tishkevich et al., 2019; Dukenbayev et al., 2019)*. It is also a new synthesis method for preparation of functional material (2-6 μm mid-IR) *(Kozlovskiy et al., 2021; El-Shater et al., 2022)*. It is well known that the combination of different compounds, which have excellent electronic properties, leads to new composite materials, which have earned great technological interest in recent years *(Kozlovskiy et al., 2021; Almessiere et al., 2022)*.

Commercial cement and service of an expert panel (n:6) from a local cement manufacturing factory utilized. The spraying was done from 0.25 to 0.5 meter towards any type of packaged (polythene, paper, glass) material (e.g cement bags here) *(Method of MIRGA spraying in Supplementary file – video V1)*. This distance is essential for the MIRGA sprayed solution to form ion clouds, oscillation and 2-6 μm mid-IR generation. The mid-infrared can penetrate the intervening package and act on the cement inside. Close spraying doesn't generate energy. MIRGA is used like a body spray.

The instruments used to find the changes in,

Chemical compound transformation – gas chromatography mass spectrometry (GC-MS): Agilent technologies, 7820 GC system, 5977E MSD, Colomn DB-5, Over temp 100-270^{0}C, Detector MS, Flow rate 1.2, Carrier gas Helium.

Chemical bond changes – fourier-transform infrared spectroscopy (FTIR): JASCO FT-IR 4200 plus spectrophotometer with ATR (range 4000–400 cm^{-1} at 298 K); and IR AFFINITY I – FTIR Spectrophotometer, FTIR 7600, Shimadzu.

Structural changes – powder x-ray diffraction (PXRD): Rigaku RINT 2500 X-ray diffractometer (CuKα anode; λ = 1.541Å). Samples scanned at 40kV and

Author α: Veterinary Hospital, Gokulam Annadhanam Temple Complex, Meenavilakku-Meenakshipuram Road, Anaikaraipatty Post, Bodinayakanur Taluk, Theni Dt, Tamil Nadu, India.
e-mail: rkbuma@gmail.com
Author σ: Veterinary Hospital, Vadakupudhu Palayam, Erode Dt, Tamil Nadu, India.
Author ρ: Assistant Professor, Department of Botany, The Standard Fireworks Rajaratnam College for Women, Sivakasi, Virudhunagar (Dt), Tamil Nadu, India.

30mA from 5° to 35° 2θ values and analyzed using PDXL2 software (Rigaku).

Configuration – transmission electron microscopy (TEM): High resolution transmission electron microscopy (HR-TEM) on JEOL (JEM-2100 Plus) system under an acceleration voltage of 200 kV.

Nuclear resonances – Solid state ^{27}Al nuclear magnetic resonance: The experiments were done on a 600 MHz NMR spectrometer (ECZR Series, JEOL, JAPAN) using a 3.2mm CPMAS probe at 150MHz frequency. All the samples were run at 18KHz spinning speed at room temp and with a delay of 5sec.

a) Method 1

A commercial bag containing M20 grade 50 kg cement was purchased. From that bag, 1000gms cement was taken, transferred to a polyethene pouch (more than 51 micron thickness) and its opening sealed with cellophane. Similarly, 10 more packets prepared. Among the 11 packets, one was marked as C (Control) and the remaining 10 were individually numbered from 1 to 10. The numbered pouches were respectively given 1 to 10 MIRGA sprayings from 0.25-0.50 meter towards the pouches, at a rate of 1 or 2 on one or either side of the pouches.

Using cement from each of the 11 pouches, a standard weight of ingredients aggregate prepared, cubes of same size were individually casted. Manual casting and compaction of cubes done (pair-form-technique). The cubes were separately cured by submerging in water. Compression tests were conducted with compression testing machine 1000 KN capacity at 7, 14 and 28 days. The trials were conducted in quadruplet and CSC results were compared.

b) Method 2

M20 grade 50 kg cement bag was purchased of the same brand and batch as in method 1. 4 samples of 1000 gms each were prepared. One sample was marked as C (Control) and the remaining 3 were numbered 1, 2 and 3. MIRGA salt was added at 0.5%, 0.75% and 1% (w/w) respectively to packets 1, 2 and 3. As in method 1, cubes were prepared, subjected to CSC testing. The trials were conducted in quadruplet and results were compared.

III. Results and Discussion

a) Method I

6 and 10 times MIRGA sprayed cement cubes, on 28th day was found to have increased 38-48% CSC respectively compared to control cubes *(Table 1)*.

Table 1: Compressive Strength of Concrete (an abstract table)

Number of MIRGA spraying	Compressive Strength of Concrete in N/mm2 (method 1)			Enhanced percentage of CSC in N/mm2
	7^{th} day	14^{th} day	28^{th} day	
C (non-sprayed)	13	18	21	-
2	15	19	22	5
6	15	24	29	38
10	16	25	31	48

b) Method 2

On 28th day, the 0.75% MIRGA salt added cement cubes were found to have 38% increased CSC than control. MIRGA salt as such is a bit costlier than MIRGA sprayings.

Considering 28^{th} day results of both methods, the CSC enhancement of 38% in 6 sprayed cement sample was taken as an achievement of this research.

The sensory and other parameters of control and trialed samples given as below. These changes were observed from 1-3 minutes after MIRGA spraying.

Control: Natural texture, taste bland, soft, a pinch sank very slowly in water.

2 sprayed: Smooth texture, salty, soft, sank rapidly in water.

6 sprayed: Rough texture, more salty, course, sank very rapidly in water.

10 sprayed: Very rough texture, very salty, very course, sank very slowly in water.

Instrumentation analyses (raw data of instrumentations in Supplementary file – Data D1).

i. *GCMS*

Control: The GCMS profile of the control sample shows peaks at these retention times (min): 12.8, 13.4, 15, 16.3, 17.8, 19.7, ~19.8, ~20, and ~21.8. *2 sprayed sample:* There is one additional peak in the 2 sprayed sample at about 18.4 min compared to the control sample GCMS. This additional peak is the marker of different properties of the 2 sprayed sample. *6 sprayed sample:* There is an additional apparent peak at about 20.6 min. This change is an indicator of the rough texture, etc. of 6 sprayed sample relative to the control sample. *10 sprayed sample:* The peak at ~5.2 min in the GCMS pattern of the 10 sprayed sample does not appear in the GCMS pattern of the control sample or

other samples. This peak is the unique property of the 10 sprayed sample.

Cement sample contains many aldehydes, ketone, short chain alkane & their derivatives. After 2 spraying, there was great increment in peak of dodecane (or its derivatives) while 6 and 10 sprayings and control have not shown this peak. On contrary, 6 and 10 sprayed samples have shown the peak of Cyclohexane (or its derivatives) which was not present in 2 sprayed & control samples. In the sprayed samples, 13-Octadecenal (most abundant peak) was disappeared and converted to various derivatives depending on the number of sprayings. *(Fig 1) (Table 2)*

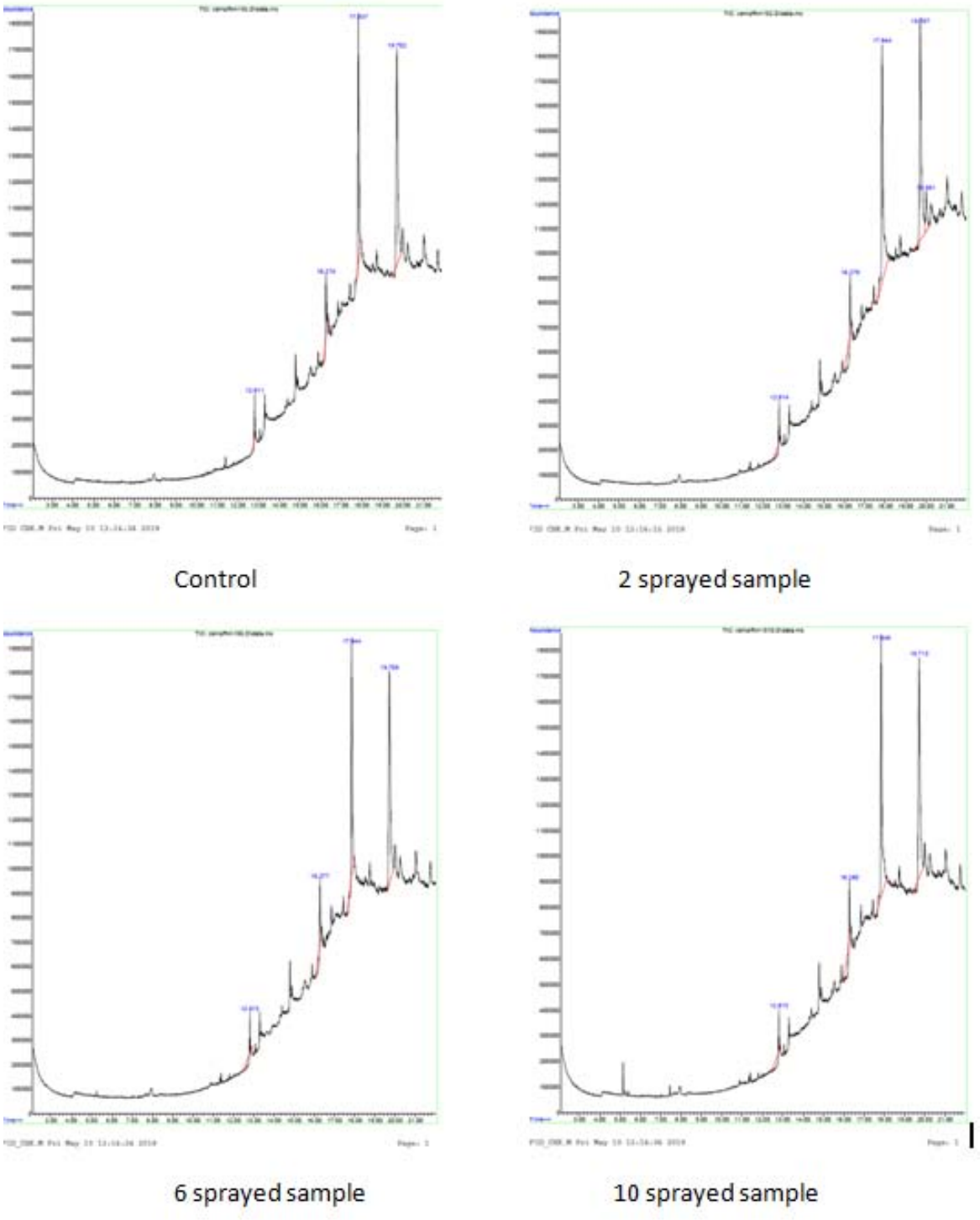

Fig. 1: GC-MS of cement samples

Table 2: GCMS spectra analysis of cement samples

R.T. (Min)	Name of Compounds in Cement	% Area presence in Sample				
		Control	2 sprayed	6 sprayed	10 sprayed	Remarks
12.809	13-Hexyloxacyclotridec-10-en-2-one	2.17	0.69	1.99	2.29	
16.270	Cyclopentadecanone, 2-hydroxy-	6.60	0.0	0.0	0.0	
16.279	13-Octadecenal, (Z)-	0.0	2.71	0.0	3.15	
16.279	2,3-Dihydroxypropyl elaidate	0.0	0.0	2.93	0.0	
17.839	Cyclopentadecanone, 2-hydroxy-	39.06	0.0	0.0	0.0	Most abundant peak in control sample
17.839	Cyclohexane, pentyl-	0.0	0.0	37.98	55.15	Most abundant peak in 10 sprayed sample
19.702	13-Octadecenal, (Z)-	52.70	0.0	0.0	0.0	Most abundant and unique peak in control sample
19.711	9-Octadecenoic acid (Z)-, 2,3-dihydroxypropyl ester	0.0	0.0	0.0	50.29	Most abundant peak in 10 sprayed sample
17.849	Dodecane, 2-cyclohexyl-	0.0	49.07	0.0	0.0	Most abundant peak in 2 sprayed sample
19.712	Cyclopentadecanone, 2-hydroxy	0.0	46.37	61.09	0.0	Most abundant peak in 6 sprayed sample
19.995	tert-Butyl(5-isopropyl-2-methylphenoxy)dimethylsilane	0.0	7.95	0.0	0.0	

ii. *FT-IR*

a. *JASCO FT-IR 4200 plus Spectrophotometer with ATR*

Control Sample: The broad signal in the range 1100-1450 cm-1 is associated with the stretching vibration of Si-OH in the silanols functional group, although observed in the fingerprint region. Furthermore, in the functional group region, the broad signal in the range 3200-3600 cm-1 is associated with the stretching vibration of O-H.

2 sprayed Sample: In the fingerprint region, the broad signal of Si-OH in the range 1100-1450 cm-1 increases significantly. Moreover, in the functional group region, there is a further broadening of O-H in the range 3200-3600 cm-1.

6 sprayed Sample: Following the same trend in the 2 sprayed sample, in the fingerprint region, the broad signal of Si-OH in the range 1100-1450 cm-1 continues increasing. Moreover, in the functional group region, the broad signal of O-H in the range 3200-3600 cm-1 increases in value.

10 sprayed Sample: In the fingerprint region, the broad signal of Si-OH in the range 1100-1450 cm-1 drops in value. In the functional group region, the broad signal of O-H in the range 3200-3600 cm-1 also drops in value.

The observed changes in the stretching vibrations of Si-OH and O-H can be interpreted as to the 2 sprayed and 6 sprayed samples being more favorable than the control sample, and the 10 sprayed sample being less favourable. At band 1623 cm-1 and 1684 cm-1 bending vibration of water in gypsum seen. At 3554 cm-1 stretching vibration of water in gypsum seen. A broad band at ~ 1650 cm-1 is due to bending vibration of irregularly bound H2O in 6 and 10 sprayed samples as the rate of hydration is more. *(Fig 2)*

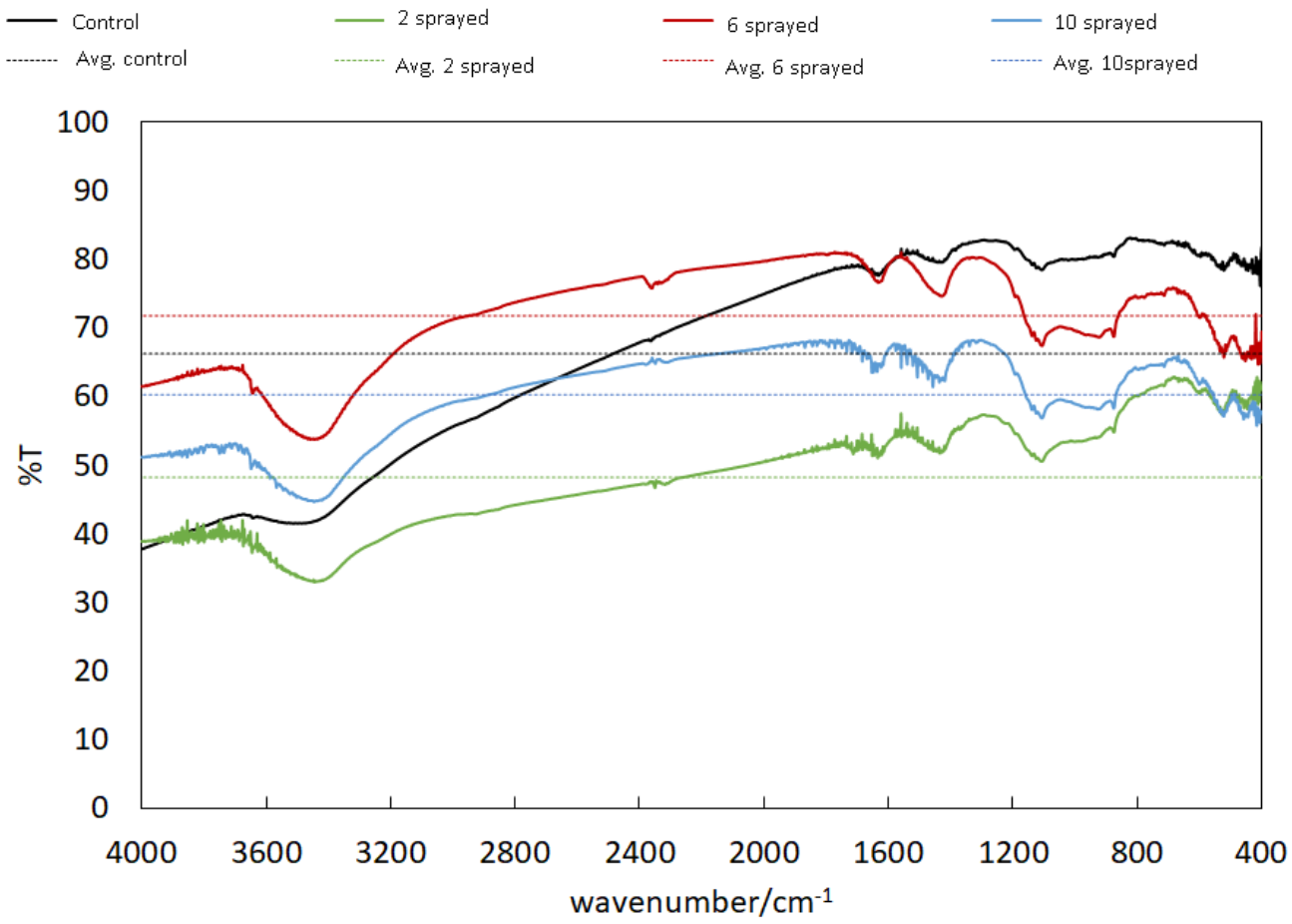

Fig. 2: FT-IR of cement

b. *IR AFFINITY I – FTIR Spectrophotometer, FTIR 7600, Shimadzu*

Cement is a mixture of different compounds. It consists of Calcium oxide (CaO), Silicon dioxide (SiO_2), Aluminum oxide (Al_2O_3), Iron oxide (Fe_2O_3), Water (H_2O), Sulfate (SO_3) and do not have any specific formula. $Ca(OH)_2$ stretch (present in control sample) indicate Portlandite of cement and it was changed in 2 and 10 sprayed samples, but disappeared in 6 sprayed sample. While10 sprayed sample showed comparatively increased C-O stretch of $[CO_3]^{2-}$, 2 sprayed sample showed high increment for Si-O stretch. The 6 and 10 sprayed samples uniquely shown asymmetric stretching of Si-O bond while S-O stretching of SO_4^{2-} was selectively present in control and 2 sprayed samples. *(Table 3) (Fig 3)*

Table 3: FTIR spectra analysis

Frequency (1/cm)	Band characteristic	% area present in each sample				
		Control	2 sprayed	6 sprayed	10 sprayed	Remarks
3417.86	Portlandite – $Ca(OH)_2$	1.39	5.34	0.0	0.75	Increase in 2 sprayed sample
1435.04	C-O stretch of$[CO3]^{2-}$	13.33	14.06	10.58	21.97	Increase in 10 sprayed sample
1103.28	S-O stretch of $[SO4]^{2-}$	6.19	5.17	0.0	0.0	Only present in control and 2 sprayed samples
1095.57	Si-O (asymmetric stretching)	0.00	0.00	3.5	6.46	Only present in 6 sprayed and 10 sprayed samples
925.83	Al-O stretch	2.14	2.22	1.44	1.76	Decrease in 6 sprayed and 10 sprayed sample
455.20	Si-O stretch	2.76	5.34	1.46	2.14	Increase in 2 sprayed sample

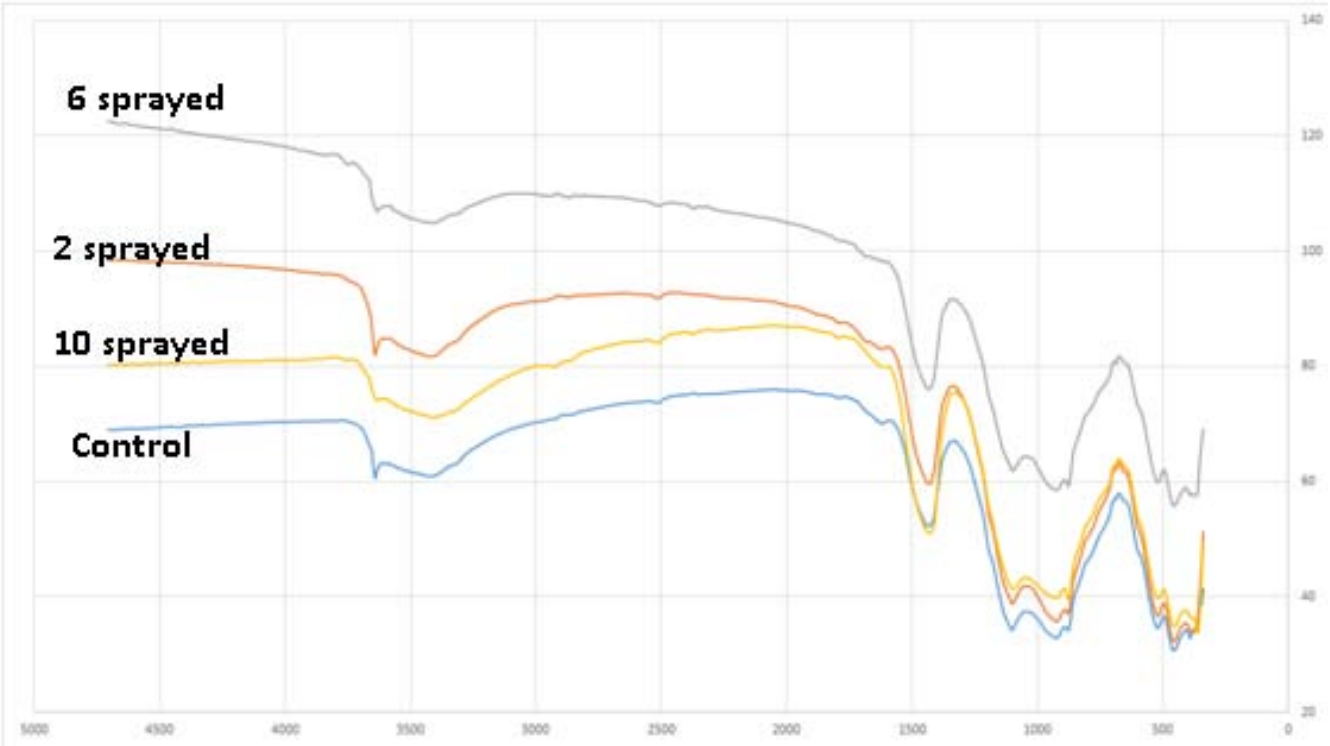

Fig. 3: FTIR of cement

iii. *PXRD*

The changes in peak intensities at 11.59° and 29.11° is due to changes in nuclear co-ordinates due to the formation of gypsum and more intense in 6 and 10 sprayed samples. The rate of hydration of the cement is increasing with the increase in the spraying number. The rate of hydration of the cement samples is in the order of control < 2 sprayed < 6 sprayed < 10 sprayed sample. *(Table 4) (Fig 4)*

Table 4: PXRD analysis

	Control		2 sprayed		6 sprayed		10 sprayed	
2θ	I	I/Imax %	I	I/Imax %	I	I/Imax %	I	I/Imax %
32.24 (Alite)	3081	100,0	3523	91,9	1911	100,0	3085	100,0
29.48 (Alite)	2837	92,1	3715	96,9	1576	82,5	2780	90,1
34.42 (Ferrite)	2582	83,8	2643	69,0	1593	83,4	2575	83,5
26.65 (Langbenite)	2418	78,5	3832	100,0	1215	63,6	2413	78,2
51.79 (Alite)	1903	61,8	1140	29,7	640	33,5	1113	36,1
18.08 (Portlandite)	1256	40,8	1321	34,5	711	37,2	1131	36,7

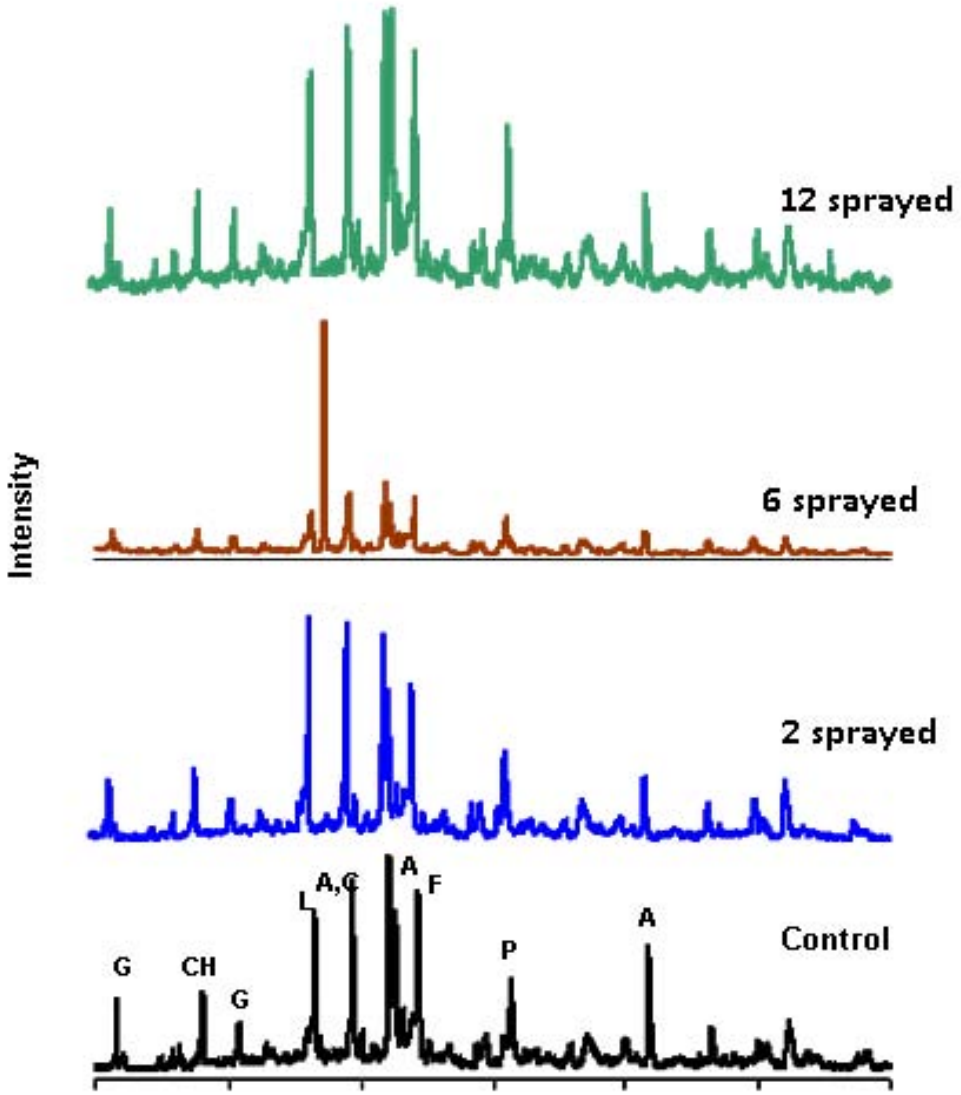

Fig. 4: PXRD of cement samples

iv. *HR-TEM*

Control sample: Mass aggregates show amorphous or ellipsoidal shape, and sizes ranging 0.4 – 1 μm. Most of these appear homogeneously dark. Bands of regularly spaced fringes suggesting Moirè patterns are visible that are typical of crystalline structures. Different particles having typical crystal shapes are visible, namely: triangular particles and needle-like particles. Concerning the triangular particles, it shows two equal-lenght sides (0.7 μm) and one shorter side (0.4 μm), recalling an isosceles triangle; it also shows bending contours at particle edges, that are typical of crystal torsions. Concerning the needle-like particles, all visible particles have same length, ranging 0.5 – 0.6 μm and show diffraction contrast evidences (including the likely Moirè patterns observed). Both types are thus compatible with crystals. Nanoparticles (average size 20 – 100 nm) are observed with prevalent squared shape and organized in clusters.

2 sprayed sample: Mass aggregates of comparable sizes and shapes organized in clusters are observed. Diffraction contrast areas are visible suggesting the presence of crystals. Different from the control, the 2 sprayed sample does not show individual particles with peculiarities typical of crystal, e.g. like those described for the control sample. Given the crystalline nature of this sample, as documented by HRTEM images, small crystals are present here, instead of large ones observed in the control. Moreover, the low frequency by which features typical of crystal structure are observed is coherent with the low frequency of areas of lattice fringe bands observed. Individual nanoparticles similar to those in the control are not visible in the 2 sprayed sample; however, in the aggregate some objects are observed which are comparable to nanoparticles observed in the control.

6 sprayed sample has different clusters of mass aggregates showing various shapes and sizes, at

increasing magnification; a cluster of rectangular crystals and a diffraction pattern image are also shown. Differently from control and 2 sprayed samples, 6 sprayed sample features typical of crystalline structures spread all over the sample mass. This sample is characterized by a large number of crystal structures. Measures of the ring radii in reciprocal lattice unit (1/nm) provide the following interplanar distances (real space, nm): 0.12, 0.16 and 0.20, comparable with measurements performed on bands of lattice fringes. In the diffraction pattern, bright spots are observed uniformly distributed along the rings, indicating that this sample has a polycrystalline texture where crystallites are random oriented; also this finding is coherent with information extracted from the HRTEM image of this sample. Sizes and shapes of mass aggregates are similar to those of control and 2 sprayed samples. However, while in aggregates of these samples diffraction contrast is observed in limited areas of the aggregate, in the 6 sprayed sample signals of diffraction contrast and of Moirè patterns are observed with very high frequency. Moirè patterns are particularly evident. Rectangular and/or squared crystals are also observed with side lengths 0.3 – 0.4 x 0.05 (μm x μm), and 110 – 130 nm respectively.

10 sprayed sample: Similarly to 6 sprayed sample, this sample features typical of crystalline structures in sample mass. This is characterized by a large number of crystal structures. Due to strong overlapping, sizes of individual crystallites are hard to be measured; however they range 50 – 130 nm approx. It has to be noted that, differently from previous samples, crystallites show ellipsoidal shape in the 15-10. Also a small squared crystal is present with side length 40 – 50 nm. Another structure is visible suggesting the presence of overlapped crystals, since dark fringes are observed suggesting diffraction contrast.

In short, degree of crystallinity increased from the control to 6 sprayings. The regularity of crystal structure is enhanced proportionally with increasing spraying from control to 10 sprayings. Concerning the regularity of the crystal structure, instead, an effective improvement is only observed from the 6 and 12 sprayed samples, due to the high degree of crystallinity observed for these two samples. *(Fig 5)*

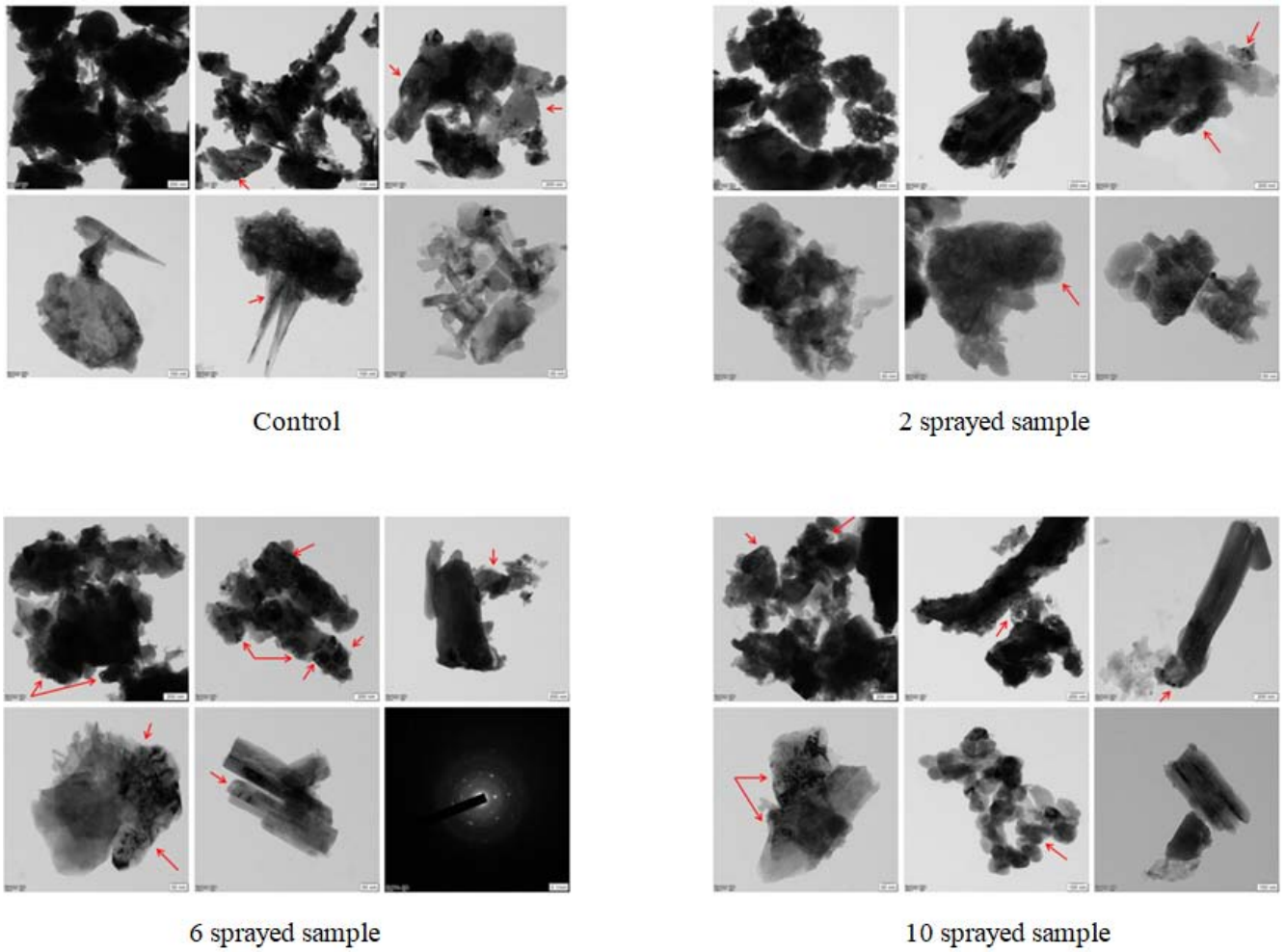

Fig. 5: HR-TEM bright field images of cement samples

v. *Solid state ^{27}Al NMR*

Since there is no significant change in the chemical shift and the integral value of the trans-1,2 disubstituted alkene–OCH3 at 130.370 ppm in control, 2, 6 and 10 sprayed samples, we used this peak as a reference to normalize the integral values in all the three data sets. With respect to the control sample, the sulfur compounds at 14.771 ppm and 61.708 ppm drop in the2 sprayed sample. But in the 6 and 10 sprayed samples theses integrals increase in value again. This behavior is concluded as the 6 and 10 sprayed samples are more favorable than control. *(Table 5) (Fig 6)*

Table 5: ^{27}Al NMR analysis

Chemical Shift Description			Control Sample			2 sprayed sample			6 sprayed sample			10 sprayed sample		
			CS	PI	NPI	CS	PI	NPI	CS	PI	NPI	CS	PI	NPI
			-100.181	0.59	1.25	-100.543	0.61	1.01	-100.543	0.62	0.98	-100.352	0.63	1.10
Sulfur Compounds	Sulfides		14.771	1.47	3.13	14.771	1.73	2.87	14.714	2.23	3.55	14.676	2.02	3.51
Sulfur Compounds	Sulfonic and Sulfinic Acids and Derivatives		61.708	8.61	18.30	61.137	8.64	14.35	61.156	9.14	14.55	61.079	9.01	15.69
trans-1,2-Disubstituted Alkenes	–OCH3	Alkenes	130.370	0.47	1.00	130.256	0.60	1.00	130.332	0.63	1.00	129.913	0.57	1.00

CS *- Chemical Shift (ppm);* ***PI*** *- Peak Integral;* ***NPI*** *- Normalized Peak Integral*

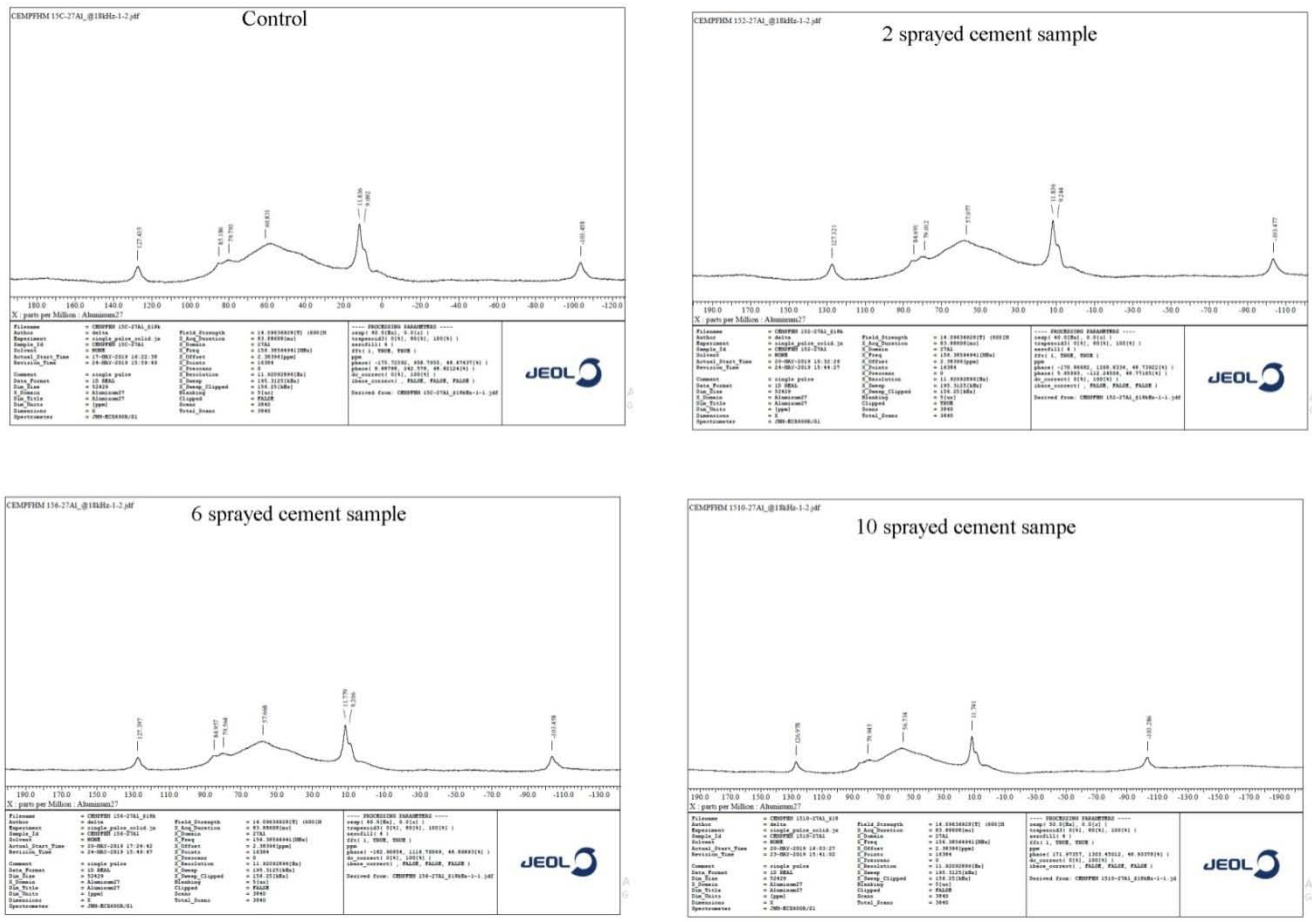

Fig. 6: NMR spectra of cement samples

To conclude, the changes in the chemical bonds thereby chemical transformation, configurational changes caused by MIRGA is the cause for inherent characteristic changes in the sprayed cement samples.

c) Future Benefits of Sprayed Cement

- Instead of 1kg of cement (1000 gm), 620 gm of MIRGA sprayed cement (as 38% CSC increased) is enough to achieve regular CSC.
- Economy saved on cements there by aggregate, water and labour also.
- Production and transport costs reduced.
- Environmental pollution and health hazards reduced.

d) Action of MIRGA Emitted 2-6 µm mid IR on Cement

Invention background, definition, technique of mid-IR generation from MIRGA, toxicological study on MIRGA, safety of the MIRGA sprayed usables and primeval and future scope of MIRGA have been described by Umakanthan *et al*., 2022a *(detailed discussion on MIRGA available in supplementary text T2)*. While spraying MIRGA, most of the mid-IR energy scatters through the air and gets absorbed by cement. Organic compounds absorb mid-IR radiation which causes a change in molecule's vibrational state to move from the lower ground state to excited higher energy state *(Girard, 2014)*. This leads to changes in cement's chemical bonds *(Shankar, 2017; Mohan, 2004)* and these bond parameter changes led to consequent changes in cement's physical and chemical characters, configuration, compound transformation depending on the dose of mid-infrared applied *(Yi, 2012; Esmaeili, 2015; Atkins, 2011; Datta et al., 2014)*.

As displayed in the results, 2-6 *µ*m MIR generated from the MIRGA equipment caused chemical and molecular level changes in the cement components (photodegradation). In this process, chemical components of the cement have absorbed the MIR and the absorbed MIR photons have altered the chemical bonds of cement molecule; thereby some of the cement molecules are degraded and transformed into another molecule/compound, as reported in GCMS analysis.

Mid-IR has unique vibrational transitions of most molecules (here cement) *(Waynant et al., 2011)* and has caused various chemical bond stretching and bendings *(Mohan, 2004; Agarwal et al., 2014)*, including new molecule formulation like gypsum formation, crystallinity and hydration *(Xu et al., 2017)*, thus lead to consequent change in physical and chemical properties of cement *(Esmaeili, 2015; Datta et al., 2014)*, hence improved CSC. Mechanical strength of cement mainly comes from accelerated hydration and chemical reaction *(Liu et al., 2020)* and also refinement of –CH crystal *(Wang et al., 2019)*. The said effects were produced by the mid-infrared as observed in the instrumentation results.

Depending on number of MIRGA spraying (energy given), a receptor's chemical bond configurations and subsequent physical and chemical characters can be altered to our desire. Such desirable results in coffee, tea, cocoa and edible salts were achieved using MIRGA spraying by *Umakanthan et al., 2022a; Umakanthan et al., 2022b; Umakanthan et al., 2023c; Umakanthan et al., 2023d.*

Since long, alternative to cement research is ongoing with merits and demerits of the results. CSC improving technologies are use of nanocements *(Brown et al., 2019)*, use of higher strength concrete (40 MPa or 50 MPa) *(Jemimah et al., 2021)*, use of metals waste *(Bacelar et al., 2022)* and mine drainage sediments, calcium sulfo-aluminate/alkaline hydroxide substances/ aluminosilicate minerals/sodium potassium silicate minerals *(Hong et al., 2016)*. CSC was also increased by various researchers by irradiation with ultraviolet *(Bo et al., 2011)*, microwave *(Dmitriev et al., 2017)*, gamma rays *(Osamu et al, 2013)*, neutron and radiation on sulphur polymer concrete *(Piotr et al., 2020)*, but these are having limitations with application and cost-effectiveness. Far-infrared rays a non-ionizing safe irradiation has also been used in CSC improvement *(Fukazawa et al., 1990)*.

Recently, cement based geopolymer materials are evolved which are technically advantageous. On contrary, cost is high, impracticable in large scale construction and unstable performance *(Liu et al., 2020)*. MIRGA technology can be placed in the literature as one of the CSC improving research.

IV. Conclusion

Mid-IR treated cast cement cubes showed 38% enhanced CSC versus non-treated. Thus, cement quantity could be reduced to 38% less than the usual requirement, saving resources and economy. If the usual quantity of cement is used, 38% more CSC would result. In the authors' opinion, this study has scope for more fruitful research on cement and its allied materials potentiation, which may result in further economy, reduced transport cost, resource saving and ecological impact.

Author Contribution

Umakanthan: Conceptualization, Methodology, Project administration, Resources, Supervision, Validation.
Madhu Mathi: Data curation, Investigation, Visualization, Writing - Original draft preparation.
Umakanthan, Madhu Mathi: Writing - Reviewing and Editing.

Competing Interest

In accordance with the journal's policy and our ethical obligation as researchers, we submit that the authors Dr.Umakanthan and Dr.Madhu Mathi are the inventors and patentee of Indian patent for MIRGA

(under-patent no.: 401387) which is a major material employed in this study.

Data and Materials Availability

All data is available in the manuscript and supplementary materials.

Funding

The authors received no specific funding for this research.

References Références Referencias

1. Liu, C., Huang, X., Wu, Y., Deng, X., Liu, J., Zheng, Z., & Hui, D. (2020). Review on the research progress of cement-based and geopolymer materials modified by graphene and graphene oxide, Nanotechnology Reviews, 9(1), 155-169. doi: https://doi.org/10.1515/ntrev-2020-0014
2. Jared L. Brown, Isaac L. Howard, and Robert Varner. Concrete compressive strength variation due to cement source change. Proceedings of the Institution of Civil Engineers - Construction Materials 2022 175:5, 213-232.
3. Umakanthan, Mathi M, 2022a. Decaffeination and improvement of taste, flavor and health safety of coffee and tea using mid-infrared wavelength rays. Heliyon, e11338, Vol 8(11). doi: 10.1016/j.heliyon.2022.e11338
4. Umakanthan T, Mathi M, 2022b. Quantitative reduction of heavy metals and caffeine in cocoa using mid-infrared spectrum irradiation. Journal of the Indian Chemical Society, Vol 100 (1). doi: 10.1016/j.jics.2022.100861
5. Tishkevich D I, Korolkov I V, Kozlovskiy A L, Anisovich M, Vinnik D A, Ermekova A E, Vorobjova A I, Shumskaya E E, Zubar T I, Trukhanov S V, Zdorovets M V, Trukhanov A V, 2019. Immobilization of boron-rich compound on Fe_3O_4 nanoparticles: Stability and cytotoxicity, J. Alloys Compd. 797, 573-581. https://doi.org/10.1016/j.jallcom.2019.05.075
6. Dukenbayev K, Korolkov I V, Tishkevich D I, Kozlovskiy A L, Trukhanov S V, Gorin Y G, Shumskaya E, Kaniukov E Y, Vinnik D A, Zdorovets M V, Anisovich M, Trukhanov A V, Tosi D, Molardi C, 2019. Fe_3O_4 nanoparticles for complex targeted delivery and boron neutron capture therapy, Nanomaterials, 494. https://doi.org/10.3390/nano9040494.
7. Kozlovskiy A L, Alina A, Zdorovets M V, 2021. Study of the effect of ion irradiation on increasing the photocatalytic activity of WO_3 microparticles, J. Mater. Sci.: Mater. Electron. 32, 3863-3877. https://doi.org/10.1007/s10854-020-05130-8
8. El-Shater R E, Shimy H E, Saafan S A, Darwish M A, Zhou D, Trukhanov A V, Trukhanov S V, Fakhry F, 2022. Synthesis, characterization, and magnetic properties of Mnnanoferrites, J. Alloys Compd. 928, 166954. https://doi.org/10.1016/j.jallcom.2022.166954
9. Kozlovskiy A L, Zdorovets M V, 2021. Effect of doping of $Ce^{4+/3+}$ on optical, strength and shielding properties of (0.5-x)TeO_2-0.25MoO-0.25Bi_2O_3-xCeO_2 glasses, Mater. Chem. Phys. 263, 124444. https://doi.org/10.1016/j.matchemphys.2021.124444
10. Almessiere M A, Algarou N A, Slimani Y, Sadaqat A, Baykal A, Manikandan A, Trukhanov S V, Trukhanov A V, Ercan I, 2022. Investigation of exchange coupling and microwave properties of hard/soft $(SrNi_{0.02}Zr_{0.01}Fe_{11.96}O_{19})/(CoFe_2O_4)_x$ nanocomposites, Mat. Today Nano, 100186. https://doi.org/10.1016/j.mtnano.2022.100186
11. Girard J E, 2014. Principles of Environmental Chemistry, 3rd edition, Jones & Bartlett Learning, USA, p99
12. Shankar D R, 2017. Remote Sensing of Soils. Germany: Springer-Verlag GmbH, p268.
13. Mohan J. Organic Spectroscopy: Principles and Applications, 2nd edition, Alpha science international Ltd., Harrow, UK, 19, (2004). Available at: *https://books.google.co.in/books?id=fA08Uy5DR0QC&printsec=frontcover&dq=Jag+Mohan.+Organic+Spectroscopy:+Principles+and+Applications&hl=en&sa=X&ved=0ahUKEwjHpcHUi9fgAhXXFIgKHXvRCpIQ6AEIKjAA#v=onepage&q=Jag%20Mohan.%20Organic%20Spectroscopy%3A%20Principles%20and%20Applications&f=false*
14. Yi G C, 2012. Semiconductor Nanostructures for Optoelectronic Devices: Processing, Characterization and Applications. Berlin, Heidelberg: Springer-Verlag, p198.
15. Esmaeili K, 2015. Viremedy, Homeopathic Remedies, and Energy Healing Remedies as Information – including Remedies; A Synopsis [Revision Aug 2015; E-pub.: Aug.2015] (First Pub: 2013). Google books, p43
16. Atkins P, Paula J, 2011. Physical Chemistry for the Life Sciences, Oxford university press, Oxford, p365
17. Datta S N, O'Trindle C, Illas F, 2014. Theoretical and Computational Aspects of Magnetic Organic Molecules. Imperial College Press, London, p224
18. Waynant R W, Ilev R K, Gannot I, 2001, Mid-infrared laser applications in medicine and biology. Phil. Trans. R. Soc. Lond. A, 359, 635-644.
19. Agarwal C M, Ong J L, Appleford M R, Mani G, 2014. Introduction to Biomaterials: Basic Theory with Engineering Applications. Cambridge university press, UK, p81.
20. Xu R, Xu Y, 2017. Modern Inorganic Synthetic Chemistry, 2nd edn., Elsevier B.V, Netherlands, UK, USA, p124.
21. Wang Q, Li S, Pan S, Cui X, Corr D, Shah S. (2019). Effect of graphene oxide on the hydration and microstructure of fly ash-cement system.

Construction and Building Materials. 198. 106-119. 10.1016/j.conbuildmat.2018.11.199.
22. Umakanthan, T, Mathi, M, 2023c. Increasing saltiness of salts (NaCl) using mid-infrared radiation to reduce the health hazards. Food Science & Nutrition, 00, 1–15. https://doi.org/10.1002/fsn3.3342
23. Umakanthan, Madhu Mathi, 2023d. Potentiation of Siddha medicine using Muppu (Universal Potentiator). International Journal of Pharmaceutical Research and Applications Volume 8, Issue 4 July-Aug 2023, pp: 2070-2084.
24. Brown, J & Howard, Isaac & Varner, Robert. (2019). Concrete compressive strength variation due to cement source change. Proceedings of the Institution of Civil Engineers - Construction Materials. 175. 1-43. 10.1680/jcoma.18.00067.
25. Jemimah, C, Milton., Prince, Arulraj, Gnanaraj. (2021). Compressive Strength of Concrete with Nano Cement. doi: 10.5772/INTECHOPEN.93881
26. B.A., Bacelar., Thalita, Cardoso, Dias., Péter, Ludvig. (2022). Reduction of the environmental impacts of reinforced concrete columns by increasing the compressive strength: a life cycle approach. Revista IBRACON de Estruturas e Materiais, doi: 10.1590/s1983-41952022000600010
27. Hong, J, Hee., Ryu, Yong, Sun., Kang, Dae, Kyu. (2016). Cement composition for durability increase.
28. Bo, Z., Yong, Zhang., Jianfeng, Zhou., Li, Chen., Deli, Li., Jianguo, Tan. (2011). UV irradiation improves the bond strength of resin cement to fiber posts.. Dental Materials Journal, doi: 10.4012/DMJ.2010-179
29. M., S., Dmitriev., M., V., D'yakonov., R., A., Krasnokutskiy., A., D., Kolyaskin., S, A, Dmitriev. (2017). Influence of microwave irradiation of cement mixtures on the strength of cement stone and concrete. doi: 10.1088/1742-6596/941/1/012101
30. Osamu, K., Shohei, Sawada., Ippei, Maruyama., Masayuki, Takizawa., Osamu, Sato. (2013). Evaluation of irradiation effects on concrete structure -gamma-ray irradiation tests on cement paste-. doi: 10.1115/POWER2013-98099.
31. Piotr, S., Joanna, Celinska., Andrzej, Gasiorowski., Rafal, Anyszka., Radoslaw, Walendziak., Michal, Lewandowski. (2020). Radiation induced strength enhancement of sulfur polymer concrete composites based on waste and residue fillers. Journal of Cleaner Production, doi: 10.1016/J.JCLEPRO.2020.122563
32. Fukazawa, T., Fukazawa, Tatsuo., Watanabe, Sumio. (1990). Manufacture of concrete or mortar member.

Supplementary Material

Supplementary data D1: Raw data files of cement instrumentations
https://drive.google.com/open?id=1Q1igeEkD5YHE0TZ-aE99MFBcALmAhMu9

Supplementary video V1: Method of MIRGA spraying
https://drive.google.com/open?id=1QoRwTESKfSdoJTfD--xIG9YpTDnVonGW

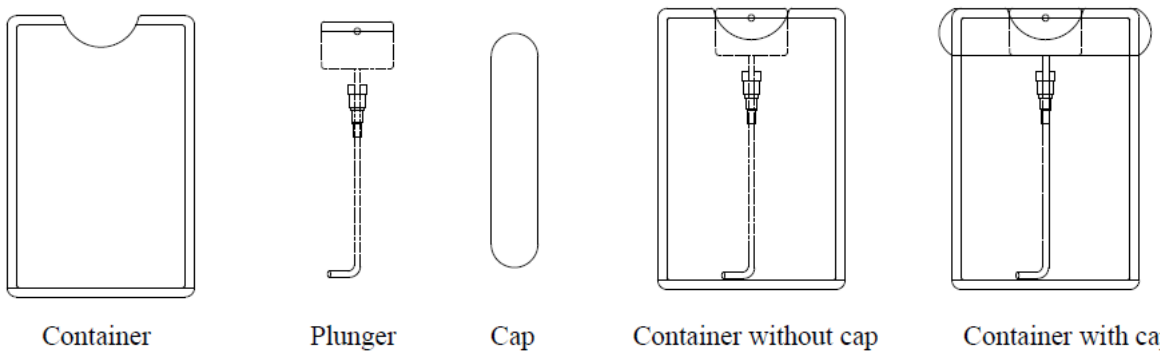

Supplementary Figure F1: MIRGA spray diagram

Supplementary Text T1: Details of MIRGA

MIRGA *(patent no.: 401387)* is a 20-mL capacity polypropylene plastic atomizer containing an inorganic (molar mass 118.44 g/mole) water-based solution in which approximately two sextillion cations and three sextillion anions are contained. The sprayer unit has dimensions 86 × 55 × 11 mm, an orifice diameter of 0.375 mm, ejection volume 0.062 ± 0.005 mL, and ejection time 0.2 s. The average pressure is 3900 Pa, and the cone liquid back pressure is 2000 N/m^2 *(Supplementary Fig (ii))*. During spraying, approximately 1-μg weight of water is lost as mist and the non-volatile material in the sprayed liquid has a concentration of 153 mg/mL. Every time spraying emits 0.06ml which contains approximately seven quintillion cations and eleven quintillion anions.

Depending on the pressure applied to the plunger, every spraying is designed to generate 2–6 μm as estimated by an FTIR (retro-reflector) interferometer instrument (Detector type D* [cm HZ1/2 - 1] MCT [2-TE cooled]) at Lightwind, Petaluma, CA, USA.

Supplementary Text T2: Detailed Discussion

1. *Detailed discussion [1]*

1.1. *Invention background*

The four observable states of matter (solid, liquid, gas, and plasma) are composed of intermolecular and intramolecular bonds. The inherent characteristics of neutrons, protons and electrons are unique, however, differences in their numbers are what constitute different atoms, and how these atoms bind together develops into different molecules with unique characteristics. In the electromagnetic wave (EMW) spectrum, the mid-IR region is vital and interesting for many applications since this region coincides with the internal vibration of most molecules [2]. Almost all thermal radiation on the surface of the Earth lies in the mid-IR region, indeed, 66% of the Sun's energy we receive is infrared[3] and is absorbed and radiated by all particles on the Earth. At the molecular level, the interaction of mid-IR wavelength energy elicits rotational and vibrational modes (from about 4500–500 cm^{-1}, roughly 2.2 to 20 microns) through a change in the dipole movement, leading to chemical bond alterations [4].

During our research we have observed: (A) In all objects, even though atoms always remain as atoms, their chemical bond parameters are continuously prone to alteration by cosmic and physical energies (e.g.: EMW, heat, pressure, and humidity) causing the bonds to compress/stretch/bend [5-8], break [9,10], or new bonds to be formed [11]. These alterations ultimately lead to changes in the physicochemical characteristics of the objects. (B) The dynamic, constant, and mutual influences of EMW among the Earth and the celestial and living bodies are continuously causing alterations in the inherent physiochemical characters of earthly objects, for instance, enhancement due to an optimum dose of energy or decrease/destruction due to a high dose of energy (detailed below). Thus, based on these concepts, MIRGA was developed to alter the bond parameters, thereby potentiating the natural characteristics of products.

1.2. *MIRGA definition*

We define MIRGA as *'a harmless, economical atomizer containing an imbalanced ratio of ions suspended in water, which influence the natural potency of target substances by generating mid-IR while spraying'*.

1.3. *Technique of mid-IR generation from MIRGA*

We designed MIRGA as to accommodate an imbalanced ratio of ions suspended in water in their fundamental state, which can move as free particles. The solution exhibits very little detectable background frequency, below even that of cosmic events. By comparison humans emit more radioactivity (around 10 microns) [12,13]. We designed MIRGA to generate energy based on various processes such as: (A) spraying leads to ionization (electrons getting separated from atoms) and many pathways for electron re-absorption; due to these two oscillatory processes, energy is generated; (B) while spraying, a water-based ionic solution gets excited/charged, which in turn leads to oscillation among the imbalanced ions [14] in their excited state, resulting in the emission of photons [15,16]; (C) although a low electromagnetic field exists between the charged particles of the MIRGA's ionic solution, during spraying the induced oscillation between these charged particles produces energy [17-21]; and (D) in the natural rainfall process, more energy is required to break the water bonds for creating smaller water droplets [22]. Therefore, these droplets should have more stored energy, which then travels down at velocity from a specific distance, thus gaining kinetic energy. When the rain hits the Earth's surface, it forms a very thin film of mid-IR (nearly 6 micron), hence there is a net heat gain [22,23]. We simulated this rainfall's energy-gaining process in MIRGA (i.e., when imbalanced ions in liquid media are atomized, the ejected smaller droplets should have higher internal energy as well as acquired kinetic energy, and the energy emitted by breaking the surface tension). From trial and error, we calibrated the ejection pressure to obtain a desired fine mist, and minimized the evaporation rate by altering the pH and density of the solution. Moreover, the accelerated ions in the sprayed ionic clouds collide among themselves and generate energy [24], thus, we incorporated these phenomena in our atomizer and designed it in such a way as to emit energy in the 2–6 μm mid-IR depending on the given plunger pressure.

Yousif et al. [25] described this process as a photodissociation of molecules caused by the absorption of photons from sunlight, including those of infrared radiation, visible light, and ultraviolet light, leading to changes in the molecular structure.

1.4. *Safety of MIRGA-sprayed products*

In our nearly two-decades of research, we have observed that MIRGA-induced bond-altered target substances do not show any adverse reaction upon consumption/use. In nature, (A) Stereochemical configuration has great influence on taste [26] (e.g., varieties of mango, grapes, rice, etc.), (B) Cooking and digestive enzymes break chemical bonds, thereby softening foods. This indicates that alterations in chemical bonds occur naturally and do not represent a risk to human health. As an example, boiled rice, puffed rice, flat rice, and rice flour have a unique aroma, taste,

texture, and shelf-life but conserving the same molecular formula ($C_6H_{10}O_5$). (C) In the food industry, sensory attributes and shelf-life are enhanced by altering the food's chemical bonds using various irradiation processes like radappertization, radicidation, and radurization [27]. (D) Upon heating, water changes from ice to liquid to steam, which are manifestations of changes in the hydrogen bonds [28] but the chemical composition (H_2O) remains the same [29].

1.5. *MIRGA's primeval and future scope*

The water-based MIRGA could be the first novel potentiating technology. This type of atomizer technology also seems to be present with the extra-terrestrials for their therapeutic use during visitations [30].

In various products, we have achieved a range from 30% to 173% potentiation. Even the smaller improvement resulted in 30% monetary and resource savings as well as health benefits. However, there is a knowledge gap between potentiation from 30% to at least 100% for all products, which can be filled-up by refining MIRGA's ionic solution, concentration, atomizer pressure, and other parameters and even formulating a better solution.

Various mid-IR emitters are now available (e.g., silicon photonic devices [31], cascade lasers quantum and interband [32], non-cascade-based lasers, chalcogenide fiber-based photonic devices [33], and suspended-core tellurium-based chalcogenide fiber photonic devices [34]). These emitters are not as cost-effective as MIRGA and are useful only in astronomy, military, medicine, industry, and research applications. These emitters are too complex for domestic application by the average user.

Because of MIRGA's wide range of applications, we believe that this technique will resonate in many scientific fields including biophotonics, therapeutics, health, ecology, and others. We are currently conducting research on MIRGA and its applications, namely MIRGA salt, MIRGA vapor and MIRGA plasma.

References Références Referencias

1. Umakanthan, Mathi M, 2022. Decaffeination and improvement of taste, flavor and health safety of coffee and tea using mid-infrared wavelength rays. Heliyon, e11338, Vol 8(11). doi: 10.1016/j.heliyon.2022.e11338
2. CORDIS, European commission. New advances in mid-infrared laser technology, Compact, high-energy, and wavelength-diverse coherent mid-infrared source. Available at: https://cordis.europa.eu/project/rcn/99977/brief/en (last accessed on 27.01.2019).
3. A. Salam, A. Ammar, A.H. Asaad, L. Yi-Chen, C. Francesco, 2019. Molecules A Comprehensive Review on Infrared Heating Applications in Food Processing. Molecules. 24, 2-21. doi: 10.3390/molecules24224125
4. J. E. Girard, Principles of Environmental Chemistry, third ed., Jones & Bartlett Learning, USA, 2014, pp. 99.
5. James E. Girard, 2014. Principles of Environmental Chemistry, 3rd edition, Jones & Bartlett Learning, USA, p99.
6. Avelion Alvarez and Miguel Prieto, 2012. Fourier Transform Infrared spectroscopy in Food Microbiology, Springer Science & Business Media, p3.
7. Brian C. Smith. Infrared Spectral Interpretation: A Systematic Approach, CRC Press, LLC, 7, (1999).
8. Dwivedi Ravi Shankar, 2017. Remote Sensing of Soils. Germany: Springer-Verlag GmbH, p268.
9. Jag Mohan. Organic Spectroscopy: Principles and Applications, 2nd edition, Alpha science international Ltd., Harrow, UK, 19, (2004). Available at: https://books.google.co.in/books?id=fA08Uy5DR0QC&printsec=frontcover&dq=Jag+Mohan.+Organic+Spectroscopy:+Principles+and+Applications&hl=en&sa=X&ved=0ahUKEwjHpcHUi9fgAhXXFIgKHXvRCpIQ6AEIKjAA#v=onepage&q=Jag%20Mohan.%20Organic%20Spectroscopy%3A%20Principles%20and%20Applications&f=false
10. Carolyn McMakin, 2011. Frequency specific Microcurrent in pain management E-book, Elsevier, China, p 30.
11. David Moss, 2011. Biomedical Applications of Synchrotron Infrared Microspectroscopy: A Practical Approach, Royal Society of Chemistry, UK, p 58.
12. Peter H. Raven, Linda R. Berg, David M. Hassenzahl, 2012. Environment, John Wiley & Sons, Inc., USA, p45. Available at: https://books.google.co.in/books?id=QVpO2R51JBIC&pg=RA1-PA45&dq=electromagnetic+waves+make+form+new+bonds&hl=en&sa=X&ved=0ahUKEwiTnO2amMbjAhUJ3o8KHSfkAJEQ6AEIMjAB#v=onepage&q=electromagnetic%20waves%20make%20form%20new%20bonds&f=false
13. Frances Ashcroft, 2000. Life at the Extremes: The Science of Survival, University of California Press, California, p122.
14. Robert H. Sanders, 2014. Revealing the Heart of the Galaxy, Cambridge University Press, USA, p70.
15. Frank Verheest. Waves in Dusty Space Plasmas, Kluwer Academic Publishers, Netherlands, 89, (2000).
16. Sun Keping, Gefei Yu. Recent developments in Applied Electrostatics (ICAES2004): Proceedings of the Fifth International Conference on Applied Electrostatics, Elsevier Ltd., UK, p87.
17. Pierre L. Fauchais, Joachim V. R. Heberlein, Maher I. Boulos. Thermal Spray Fundamentals From

Powder to Part. Springer Science & Business Media, New York, 84 (2014).
18. Manfred Wendish, Jean-Louis Brenguier. Airborne Measurements for environmental Research: Methods and Instruments, Wiley-VCH. Available at: https://books.google.co.uk/books?id=tHdwhn-c5mgC&pg=PT419&dq=A+regularly+oscillating+charge+produces+a+harmonic+electromagnetic+waves+Manfred&hl=en&sa=X&ved=0ahUKEwjBqdv75tvgAhWpSxUIHbQ_D0gQ6AEIKjAA#v=onepage&q=A%20regularly%20oscillating%20charge%20produces%20a%20harmonic%20electromagnetic%20waves%20Manfred&f=false (last accessed on 27.02.2019).
19. Kongbam Chandramani Singh, 2009. Basic Physics, PHL Learning Private Limited, New Delhi, p413.
20. Mathura Prasad. Soul, God and Buddha in Language of Science, Notion Press, Chennai (2017).
21. Stephen Pople, 1999. Complete Physics, Oxford University Press, Oxford, p166.
22. Roger Barry, Richard Chorley, 1998. Atmosphere, Weather and Climate, 7th edition, Routledge, London, p51.
23. Eniday: https://www.eniday.com/en/sparks_en/harnessing-the-energy-of-rain/ (last accessed on 06.02.2019).
24. Krishnakumar, T (2019). Application Of Microwave Heating In Food Industry. 10.13140/RG.2.2.27035.72488
25. Yousif, E., & Haddad, R. (2013). Photodegradation and photostabilization of polymers, especially polystyrene: review. SpringerPlus, 2, 398. https://doi.org/10.1186/2193-1801-2-398
26. Kenneth L., Williamson, Katherine M. Masters, 2011. Macroscale and Microscale Organic Experiments, 6th edition, Brooks/Cole C engage learning, CA, p720.
27. Sivasankar B. Food Processing and preservation, PHI Learning Private Limited, Delhi, 246, (2014).
28. Trevor Day, 1999. Ecosystems: Oceans. Routledge Taylor & Francis Group, London and New York, p44.
29. Kenneth W. Raymond, 2010. General Organic and Biological Chemistry, 3rd edition, John Wiley & Sons, Inc., USA, p176.
30. Blue planet project: Alien Technical research–25, Westchester Camp, Office of the Central Research #3.CODE: ARAMISIII–ADR3-24SM, p80-81.
31. CMOS Emerging Technologies. CMOSET 2012: Abstracts, p49. Available at: https://books.google.co.in/books?id=3XVYC-yBgksC&pg=PA49&dq=mid+infra#v=onepage&q&f=false
32. Jung, D., Bank, S., Lee, M. L., & Wasserman, D. (2017). Next-generation mid-infrared sources. Journal of Optics, 19(12), 123001. doi:10.1088/2040-8986/aa939b
33. Sincore, A. & Cook, Justin & Tan, Felix & El Halawany, Ahmed & Riggins, A. & McDaniel, S. & Cook, G. & Martyshkin, Dmitry & Fedorov, V. V. & Mirov, Sergey & Shah, L. & Abouraddy, A. & Richardson, M. & Schepler, Kenneth. (2018). High power single-mode delivery of mid-infrared sources through chalcogenide fiber. Optics Express, 26(6), 7313. doi:10.1364/oe.26.007313
34. Wu, Bo & Zhao, Zheming & Wang, Xunsi & Tian, Youmei & Mi, Nan & Chen, Peng & Xue, Zugang & Liu, Zijun & Zhang, Peiqing & Shen, Xiang & Nie, Qiuhua & Dai, Shaocong & Wang, R.P. (2018). Mid-infrared supercontinuum generation in a suspended-core tellurium-based chalcogenide fiber. Optical Materials Express, 8(5), 1341. doi:10.1364/ome.8.001341